Kinetic Study, Modeling and Simulation of Homogeneous Rhodium-Catalyzed Methanol Carbonylation to Acetic Acid

Golhosseini Bidgoli, Reza; Naderifar, Abas*+

Faculty of Chemical Engineering, Amirkabir University of Technology, Tehran, I.R. IRAN

Mohammadrezaei, Ali Reza; Jafari Nasr, Mohammad Reza

Petrochemical Research & Technology Company (NPC-RT), Tehran, I.R. IRAN

ABSTRACT: *Thermodynamic restrictions and simultaneous effects of operational conditions on the homogeneous rhodium-catalyzed carbonylation of methanol are studied in this line of research. It is shown that the general NRTL-Virial model can be appropriated to study thermodynamics of the carbonylation. It is obtained that the reaction is kinetically and thermodynamically reasonable at temperatures above 420K and below 520K, respectively. Moreover, at carbon monoxide partial pressures above 10 bar, the reaction rate is independent of the partial pressure. These results are in full accord with those reported in the literature. In addition, $P_{CO} > 2$ bar is necessary for initializing the reaction. The parameters involved in the rate expression, equilibrium constants, CO solubility, and rate constant, are determined. The equilibrium constants are calculated with B3LYP/SDD ab initio method, and the value of Henry's coefficient for CO (H_{CO}) is determined as a function of temperature and methyl acetate conversion. The results predicted by this function agree well with those proposed by the general NRTL-Virial model with the errors below 11%. The Variation of CO solubility with acetic acid and methyl acetate concentrations is in good agreement with that obtained by others. It is found that the determined parameters give satisfactory predictions in modeling and simulation of the reaction.*

KEY WORDS: *Kinetic study, Modeling, Simulation, Homogeneous methanol carbonylation, Rhodium, ab initio method.*

INTRODUCTION

Acetic acid, an important industrial product, is widely used as a raw material for the production of Vinyl Acetate Monomer (VAM) and acetic anhydride. It is also used as a solvent for Purified Terephthalic Acid (PTA) produ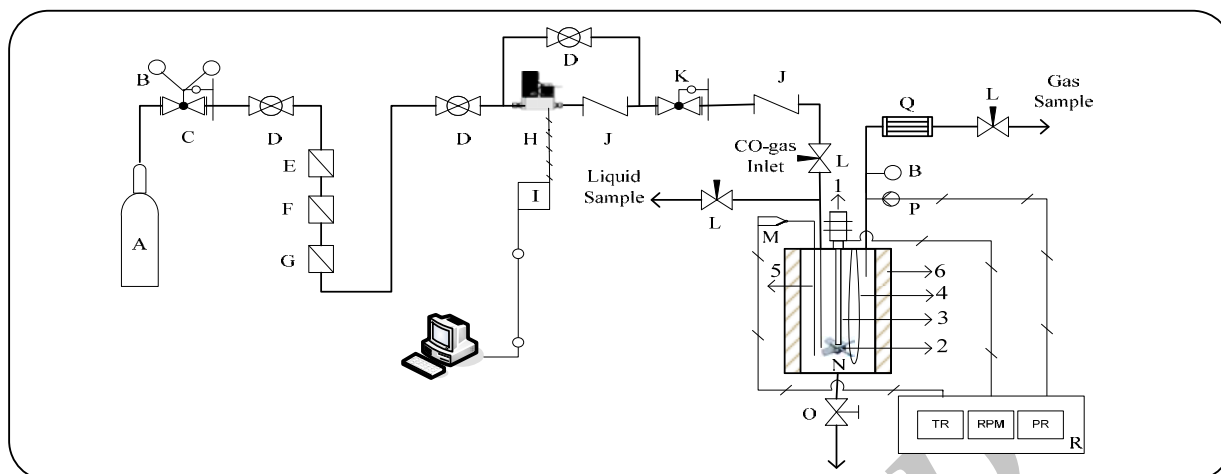ction. Though various routes for synthesis of acetic acid are known, the most important route for large-scale manufacturing of acetic acid is homogeneous methanol carbonylation through the chemical Eq. (1). The Monsanto process (Rh: catalyst; CH$_3$I: promoter; 423 - 473K; 30 - 60 bar), which is a high selective methanol

Fig. 1: Schematic diagram of the experimental set-up for methanol carbonylation: (A) CO gas cylinder, (B) pressure gage, (C) pressure regulator, (D) ball valve, (E) gas filter, (F) gas drier, (G) CO_2 adsorber, (H) mass flow meter, (I) data acquisition card, (J) check valve, (K) constant pressure regulator, (L) needle valve, (M) thermocouple, (N) autoclave of 6.35 cm diameter and 15.24 cm length (1: magnetic drive stirrer, 2: four-blade 45° pitched turbine impeller of 3.4 cm diameter, 3: stirrer shaft of 14 cm length, 4: water-cooling loop, 5: thermowell, 6: electric heating mantle), (O) discharge valve, (P) pressure transducer, (Q) double pipe condenser, (R) Parr 4843 temperature controller (TR: temperature controller and indicator, RPM: rpm indicator and manual adjuster, PR: pressure indicator).

carbonylation process (> 99% based on methanol) using water contents of 14 - 15 wt. %, was discovered in 1970s [1-3]. The main problems with the Monsanto process are the catalyst precipitation under low CO pressures and the downstream separation costs related to high water content to achieve higher activity and selectivity. On the contrary, this high water content increases the by-products formed through water gas shift reaction

$$CH_3OH + CO \rightarrow CH_3COOH \qquad (1)$$

Based on the Monsanto process, Celanese Corporation and Daicel Chemical Industries used lithium and sodium iodide promoters (ca. 20 wt. %) to carry out methanol carbonylation at low water concentrations about 2 wt. % [4-5]. In recent studies [6-8], in the low water carbonylation of methanol to acetic acid, the use of new promoters with low contents (ca. 0.3 - 4 wt. %) has been studied.

Although methanol carbonylation has been studied in literature and its mechanism is well-established [9], this study led to useful results that were mostly ignored by researchers including a comprehensive and systematic study of simultaneous effects of operating conditions and the thermodynamic restrictions on the reaction. It should be noted that the rate constant will be seriously in error if the independency of the rate data on the CO partial

pressure and on the thermodynamic restrictions is not taken into account.

The determination of reaction rate parameters, equilibrium constants, CO solubility and rate constant, can give rise to develop a reaction rate expression that could be used to design and to scale up the process. So can the study of the determined parameters in the reaction modeling and simulation by commercial simulators such as HYSYS.Plant. Because of the lack of information on homogeneous catalysts in this field, this study focuses on the kinetics of the homogeneous Rh-catalyzed methanol carbonylation (CH_3I: promoter; water content: ~ 11 wt. %) using experimental tests and applying theoretical methods such as ab initio method with the help of Gaussian-98 program.

In the following section, the experimental apparatus of the research are discussed. Then, the kinetics, modeling and simulation of the carbonylation of methanol are developed.

EXPERIMENTAL SECTION

The schematic diagram of the system used in this study is shown in Fig. 1. The experiments were performed in a semi-batch manner and carried out by using a 450 cm^3 hastelloy C autoclave (Model 4562, Parr Instrument Co., Moline, IL), equipped with a magnetically driven stirrer

with a four-blade 45° pitched turbine impeller of 3.4 cm diameter and a variable speed motor allowing for speeds up to 1300 rpm along with liquid injection facility and an internal water-cooling loop. The equipment was provided with an automatic temperature control and a pressure transducer with a precision of ±7 kPa. The temperature of the liquid in the reactor was controlled within ±1K. The catalyst (RhCl$_3$.3H$_2$O) was analytical reagent grade and was purchased from Merck. Methyl acetate (MeOAc) as the substrate, acetic acid (AcOH) as the solvent for reaction and methyl iodide as promoter with a purity above 98%, procured from Merck, were used as received. A carbon monoxide supply (99.5%, Linda) to the autoclave was provided from a reservoir.

Reaction rate is determined from the consumption rate of CO which is frequently used to run a kinetic study or check the activity of the employed catalyst in a gas-liquid system in the literature [10-12]. In a typical carbonylation experiment, the autoclave was charged with 250 grams of reaction solution in Table 1. After sealing, the autoclave was pressure tested and purged three times with 3 - 5 bar of CO. The reactor pressure was then raised to 5 bar, and by slow stirring (150 rpm), was heated to the specified temperature. Once the reaction temperature was reached, the autoclave was pressurized to the specified pressure. The autoclave stirred at 1000 - 1300 rpm in order to ensure that the gas-liquid mass transfer effects are negligible on the catalytic reaction and the kinetic regime since increasing the agitation speed from 800 to 1300 rpm showed no changes in the initial rate of reaction (Fig. 2) at different pressures (19.5 and 39 bar) and temperatures (423, 443, and 463K). Carbon monoxide consumption was measured by a mass flow meter recording the amount of CO absorption from the vessel. The mass flow meter signal was transmitted to an acquisition card (analog device) and recorded on-line by a PC. The reaction temperature was maintained at the desired value by connecting a heating mantle to the temperature control system. The reaction was carried out until CO absorption stopped completely indicating complete conversion of the substrate (MeOAc).

The possible changes in the initial reaction mixture due to the thermodynamic restrictions (vapor-liquid and chemical equilibrium) and the vapor pressure of the mixture at the different operating conditions are ignored momentarily. It means that the concentrations of the

Table 1: Operating conditions for the carbonylation reaction.

| Operating Parameters	Range
Temperature (K)	393 - 483
Pressure (bar)	19.5 - 39
Catalyst, Rh (mol)	7.105×10^{-4}
Methyl iodide (mol)	0.247
Methyl acetate (mol)	0.913
Acetic acid (mol)	2
Water (mol)	1.463
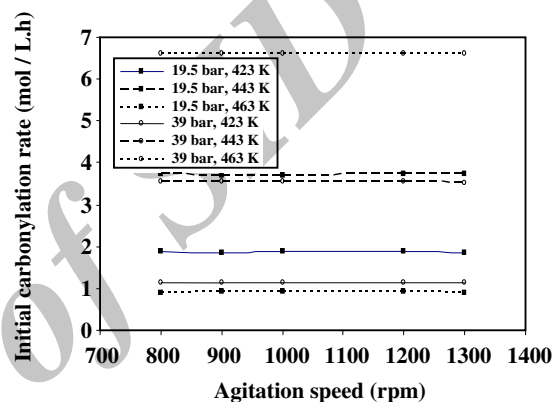
Fig. 2: Effect of the agitation speed on the initial rate of carbonylation. Reaction conditions: methyl iodide, 0.247 mol; acetic acid, 2 mol; methyl acetate, 0.913 mol; water, 1.463 mol; catalyst, 7.105×10^{-4} mol.

initial reaction mixture under the different operating conditions in kinetic study are assumed to remain unchanged.

REACTION RATE EXPRESSION

Forster [13] investigated the mechanism of methanol carbonylation reaction showing an active catalytic species [Rh(CO)$_2$I$_2$]$^-$, species A, as evidenced by in situ IR spectroscopy (Fig. 3). Oxidative addition of methyl iodide to the species A to form methyl rhodium species B is proposed to be the rate-determining step in this reaction [14]. Methyl iodide is formed from methanol and HI by chemical equation (2) presented in Fig. 3. It can also be shifted to reductive elimination step at low concentrations of water less than 8 wt. % [15] and to ligand addition at P$_{CO}$ < 10 bar [10].

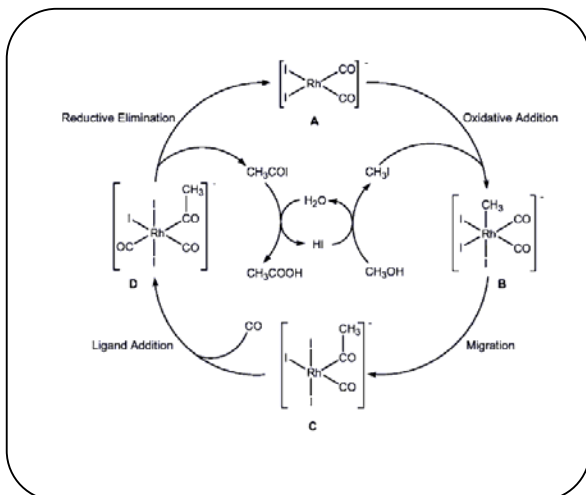$$CH_3OH + HI \leftrightarrow CH_3I + H_2O \qquad (2)$$

59
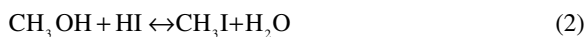
Fig. 3: Forster's mechanism for rhodium catalyzed methanol carbonylation.

At water concentrations above 8 wt.%, the dependence of the carbonylation rate on the rhodium catalyst and on methyl iodide concentration is shown in Eq. (3) [15, 16].

$$\text{Rate} \propto [\text{Catalyst}][\text{CH}_3\text{I}] \tag{3}$$

Hjortkjaer & Jensen [17] discovered that the carbonylation rate is independent of the CO pressure above approximately 2 atm. *Nowicki et al.* [11] reported that there is no direct effect of partial pressure of CO above 2 bar on the raction rates, and *Dake et al.* [10] discerned that the reaction rate in acetic acid medium is independent on the methanol concentration and not affected by the CO pressures above 10 bar in acetic acid or aqueous medium. It was also cited that the rate is independent of water content above 8 wt. % and methyl acetate content above ~1 wt. % [15].

Assuming that the oxidative addition is the rate controlling step, the carbonylation rate dependence in acidic media on the rhodium catalyst and promoter concentrations is expressed by Eq. (4) [17]. This has been used for initial rate calculation [11, 17] and is not appropriate for predicting the rate-time and the concentration-time profiles in a batch or a semi-batch reactor such as the autoclave used in this work.

$$\text{Rate} = k[\text{Rh}][\text{I}] \tag{4}$$

where k is the rate constant, and here promoter concentration ([I]) is equal to the initial concentration of methyl iodide; i.e., $[\text{I}] = [\text{CH}_3\text{I}]$.

Furthermore, in this case a general form of rate expression according to Eq. (5) was reported with consideration of assumption (7)-(9) regarding Fig. 3 [12]. The exact determination of the parameters involved in this equation can lead to reactor design, control and simulation.

$$\text{Rate} = \frac{kK'[\text{Rh}][\text{I}]_t\,[\text{CH}_3\text{OH}]}{[\text{H}_2\text{O}] + K'[\text{CH}_3\text{OH}] + K[\text{CH}_3\text{COOH}][\text{I}]_t} \tag{5}$$

$$K = (\frac{1}{K_2 K_3 K_4 K_5 [\text{CO}]} + \frac{1}{K_3 K_4 K_5\,[\text{CO}]} + \frac{1}{K_4 K_5}) \tag{6}$$

$$\text{Rate} = k[\text{A}][\text{I}]_t \tag{7}$$

$$[\text{Rh}] = [\text{A}] + [\text{B}] + [\text{C}] + [\text{D}] \tag{8}$$

$$[\text{I}]_t = [\text{CH}_3\text{I}] + [\text{HI}] \tag{9}$$
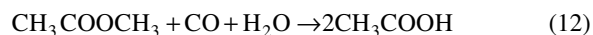
where K_2, K_3 and K_4 are the equilibrium constants of the migration, ligand addition and reductive elimination step, respectively. In addition, K' is the equilibrium constant of the chemical equation (2) and K_5 is the equilibrium constant of the production release reaction (chemical equation (10)) which is shown in Fig. 3. $[\text{I}]_t$ is the total amount of promoter equal to the initial concentration of methyl iodide in this study.

$$\text{CH}_3\text{COI} + \text{H}_2\text{O} \leftrightarrow \text{CH}_3\text{COOH} + \text{HI} \tag{10}$$

Taking methanol as the main feedstock of the experiments, the GC analysis of the liquid sample drown after heating the reactor to the reaction temperature indicates that the methanol is converted to methyl acetate through esterification (chemical Eq. (11)) with acetic acid and then carbonylated as cited in the literature [17, 18].

$$\text{CH}_3\text{COOH} + \text{CH}_3\text{OH} \leftrightarrow \text{CH}_3\text{COOCH}_3 + \text{H}_2\text{O} \tag{11}$$

Considering methyl acetate hydrolysis reaction, the reverse reaction of esterification and the chemical Eq. (1), methyl acetate can be considered as main feedstock for the carbonylation reaction (Table 1). Hence, the overall reaction can be represented as:

$$\text{CH}_3\text{COOCH}_3 + \text{CO} + \text{H}_2\text{O} \rightarrow 2\text{CH}_3\text{COOH} \tag{12}$$

In this case, the reaction rate (Eq. (5)) is expressed by Eq. (13), where K" is the equilibrium constant of the hydrolysis reaction.

$$\text{Rate}_{CH_3COOH} = \frac{d([CH_3COOH])}{dt} = \qquad (13)$$

$$\frac{kK'K''[CH_3COOCH_3][H_2O][Rh][I]_t}{([H_2O][CH_3COOH]+K'K''[H_2O][CH_3COOCH_3]+K[CH_3COOH]^2[I]_t)}$$

RESULTS AND DISCUSSION
Thermodynamic study of the reaction

The GC analysis of the liquid sample drawn after heating the reactor to reaction temperatures, 443, 463, and 483K at 34 bar, indicated that the equilibrium amount of methanol produced by the hydrolysis route (reverse of chemical Eq. (11)) is very low. The comparison of the experimental equilibrium conversion of methyl acetate to methanol with those proposed by the different property packages developed in HYSYS simulator software (Fig. 4) based upon minimizing the Gibbs free energy of the system shows that the prediction of the thermodynamic restrictions of the carbonylation system-a highly non-ideal polar system - may be governed by a dual model approach of NRTL liquid activity coefficient model and the Virial vapor phase model known as general NRTL-Virial model as a proper fluid package for multicomponent systems and extrapolation.

The binary interaction parameters of the property packages and the Virial coefficients are taken from HYSYS® library components and listed in Table 2. The mixing rule is applied through the calculation of the overall property by:

$$\text{Property}_{mix} = \sum_{i=1}^{n} x_i \, \text{Property}_i \qquad (14)$$

The dual model approach for solving chemical systems with activity models cannot be used with the same degree of flexibility and reliability as the equations of state. However, some checks such as vapor pressures can be advised to ensure a good confidence level in thermodynamic restrictions and the prediction of properties [19].

The vapor pressures of the reaction solution with and without the addition of catalyst were measured in the autoclave reactor at different temperatures and methyl acetate conversions (Figs. 5-6). In a typical experiment, the autoclave was evacuated to remove air and then charged with the reaction solution (250 grams of reaction solution presented in Table 1 based on the 0% of the
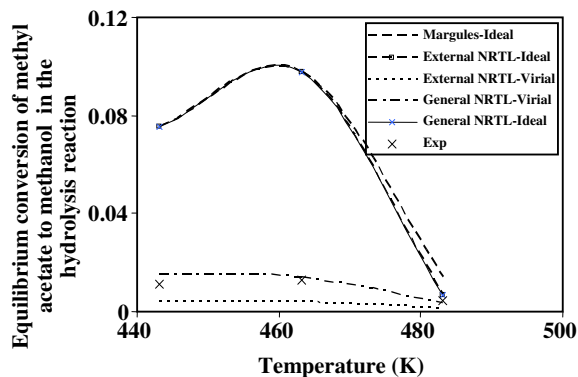

Fig. 4: Comparison of the experimental equilibrium conversion of methyl acetate to methanol with those proposed by the different property packages in the hydrolysis reaction under 34-bar pressure. (×): methyl iodide, 0.247 mol; acetic acid, 2 mol; methyl acetate, 0.913 mol; water, 1.463 mol; catalyst, 7.105 × 10⁻⁴ mol.
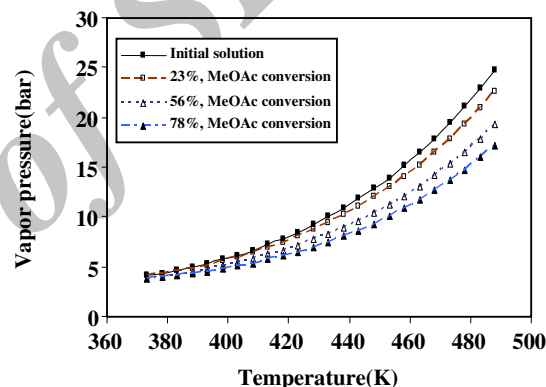

Fig. 5: Experimental vapor pressure of the reaction mixture (without catalyst) at different methyl acetate conversions and temperatures.
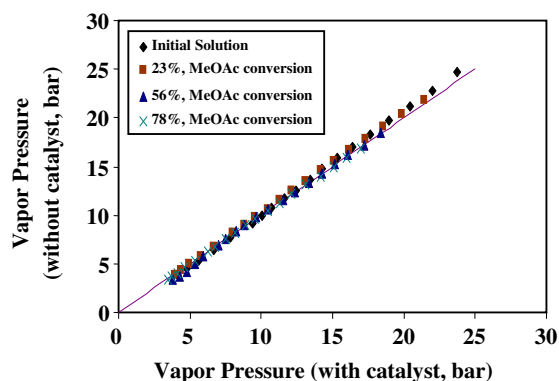

Fig. 6: Comparison of the experimental vapor pressures of the reaction mixture at different methyl acetate conversions with and without the addition of catalyst.

61

Table 2: Parameters of the property packages used in the determination of the equilibrium conversion of methyl acetate to methanol. [a]General NRTL model, [b]Extended NRTL model, [c]Margules model, [d]Virial model.

i	j	AcOH A	AcOH B	α1	MeOAc A	MeOAc B	α1	MeOH A	MeOH B	α1	CH₃I A	CH₃I B	α1	H₂O A	H₂O B	α1	CO A	CO B	α1
AcOH	a	0	0	0	0	-320.073	0.360	0	-109.290	0.305	0	0	0	0	-110.597	0.300	0	0	0
	b	0	0	0	-635.890	0	0.360	-217.126	0	0.305	0	0	0	-219.724	0	0.300	0	0	0
	c	0	0	-	0.4074	0	-	-0.4183	0	-	0	0	-	0.7819	0	-	0	0	-
	d	-	4.5	-	-	2	-	-	2.5	-	-	0	-	-	2.5	-	-	0	-
MeOAc	a	0	613.514	0.360	0	0	0	0	146.148	0.296	0	0	0	0	442.511	0.383	0	0	0
	b	1218.869	0	360	0	0	0	290.353	0	0.296	0	0	0	879.137	0	0.383	0	0	0
	c	0.003	0	-	0	0	-	1.056	0	-	0	0	-	3.121	0	-	0	0	-
	d	-	2	-	-	0.85	-	-	1.3	-	-	0	-	-	1.3	-	-	0	-
MeOH	a	0	8.379	0.305	0	223.432	0.296	0	0	0	0	0	0	0	-24.499	0.300	-4.052	-0.004	0
	b	16.646	0	0.305	443.893	0	0.296	0	0	0	0	0	0	-48.673	0	0.300	-4.052	-0.004	0
	c	-0.2101	0	-	0.9988	0	-	0	0	-	0	0	-	0.7611	0	-	0	0	-
	d	-	2.5	-	-	1.3	-	-	1.6297	-	-	0	-	-	1.55	-	-	0	-
CH₃I	a	0	0	0	0	0	0	0	0	0	0	0	0	0	0	0	0	0	0
	b	0	0	0	0	0	0	0	0	0	0	0	0	0	0	0	0	0	0
	c	0	0	-	0	0	-	0	0	-	0	0	-	0	0	-	0	0	-
	d	-	0	-	-	0	-	-	0	-	-	0	-	-	0	-	-	0	-
H₂O	a	0	424.124	0.300	0	860.466	0.383	0	307.245	0.300	0	0	0	0	0	0	-12385	0	0
	b	842.608	0	0.300	1709.488	0	0.383	610.403	0	0.300	0	0	0	0	0	0	-12385	0	0
	c	0.4748	0	-	2.110	0	-	0.6207	0	-	0	0	-	0	0	-	0	0	-
	d	-	2.5	-	-	1.3	-	-	1.55	-	-	0	-	-	1.7	-	-	0	-
CO	a	0	0	0	0	0	0	13.873	-0.029	0	0	0	0	266.360	-36.713	0	0	0	0
	b	0	0	0	0	0	0	13.873	-0.029	0	0	0	0	266.360	-36.713	0	0	0	0
	c	0	0	-	0	0	-	0	0	-	0	0	-	0	0	-	0	0	-
	d	-	0	-	-	0	-	-	0	-	-	0	-	-	0	-	-	0	-

$$a, b \quad \ln \gamma_i = \frac{\sum_{j=1}^{n} \tau_{ji} x_j \exp(-\tau_{ji}\alpha_{ji})}{\sum_{k=1}^{n} x_k \exp(-\tau_{ki}\alpha_{ki})} + \sum_{j=1}^{n} \frac{x_j \exp(-\tau_{ij}\alpha_{ij})}{\sum_{k=1}^{n} x_k \exp(-\tau_{kj}\alpha_{kj})} \left(\tau_{ij} - \frac{\sum_{m=1}^{n} \tau_{mj} x_m \exp(-\tau_{mj}\alpha_{mj})}{\sum_{k=1}^{n} x_k \exp(-\tau_{kj}\alpha_{kj})} \right), \quad c \quad \ln \gamma_i = (1-x_i)^2 (A_i + 2x_i (B_i - A_i)),$$

$$d_B = \text{second Virial coefficient (m3/mol)}.$$

where:

$$^a \quad \tau_{ij} = A_{ij} + \frac{B_{ij}}{T}, \quad \alpha_{ij} = \alpha1_{ij} . \quad (A_{ij}: cal/gmol, B_{ij}: cal\ K/gmol)$$

$$^b \quad \tau_{ij} = A_{ij} + B_{ij}(T - 273.15), \quad \alpha_{ij} = \alpha1_{ij} . \quad (A_{ij}: cal/gmol, B_{ij}: cal/gmol\ K)$$

$$^c \quad A_i = \sum_{j=1}^{n} x_j \frac{(A_{ij} + B_{ij}T)}{(1-x_i)}, \quad B_i = \sum_{j=1}^{n} x_j \frac{(A_{ji} + B_{ji}T)}{(1-x_i)} . \quad (B_{ij}, B_{ji}: 1/K$$

methyl acetate conversion and the rest conversion percentages, i.e., 23%, 56%, and 78%, based on the stoichiometry of overall reaction). After sealing, the contents were heated to the desired temperature and then stirred at 1000 rpm for about 10 min to equilibrate the liquid phase with the vapor. The changes of pressure in the autoclave were recorded on-line as a function of time until it remained constant, indicating vapor pressure of the solution. At the end of the experiments and cooling of the reactor, GC analysis of the liquid and gas phases was carried out which indicated nearly the same weight percentages of the initial liquid reaction solutions (±0.2%) and traces less than 0.5% of air in the gas phase. The weight of the reactor contents in the experiments was also nearly the same as those values of the initial solution (-1%).

Since the effect of catalyst on the vapor pressure of the reaction mixture is negligible at different temperatures and methyl acetate conversions (shown in Fig. 6), the solid catalyst is not considered in vapor pressure calculations by the general NRTL-Virial model. A good agreement between the experimental and proposed data was found (see Fig. 7) by checking the vapor pressure of the reaction mixture over different temperatures and conversions of methyl acetate.

As seen in Fig. 8, the equilibrium conversion of methyl acetate in methanol carbonylation decreases with decreasing pressure and increasing temperature, and it is also observed that there is no thermodynamic restriction on the progress of the overall reaction (chemical Eq. (12)) at temperatures below 520K and pressures used in carbonylation reaction (P > 15 bar [20-24]). It is revealed from Fig. 9 that there is no significant restriction of thermodynamic equilibrium on the progress of the esterification reaction at temperatures below 463K under the high pressures of 15, 20, 30, and 40 bar, and almost all of the methanol can be converted to methyl acetate and water. The liquid sample drawn after heating the reactor to the reaction temperatures under 15, 20, 34 and 40-bar pressures indicated that the esterification reaction proceeds completely from thermodynamic equilibrium point of view as shown in Fig. 9.

By comparing the experimental data with the results proposed by the general NRTL-Virial model shown in Figs. 8-9, the agreement was found to be excellent.
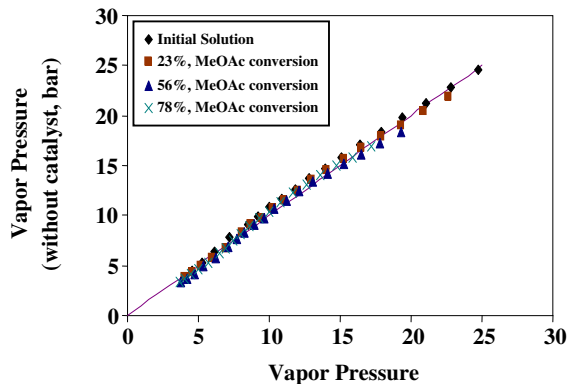

Fig. 7: Comparison of the experimental vapor pressures of the reaction mixture at different methyl acetate conversions with those proposed by the general NRTL-Virial model.
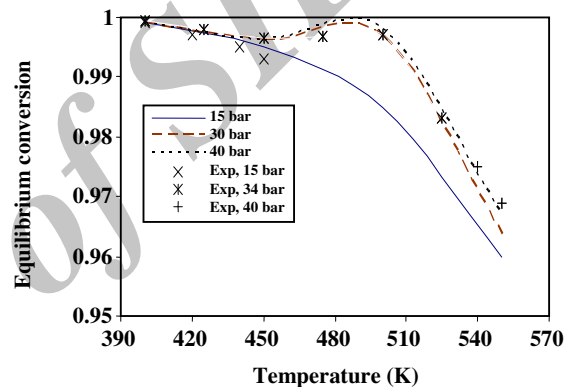

Fig. 8: Equilibrium methyl acetate conversion vs. temperature in carbonylation reaction (calculated by the general NRTL-Virial model).
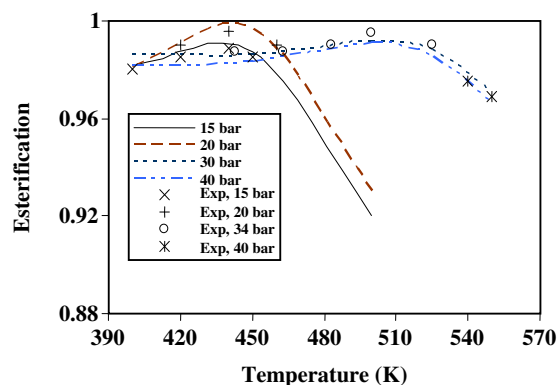

Fig. 9: Equilibrium methanol conversion vs. temperature in esterification (calculated by the general NRTL-Virial model). (×): methyl iodide, 0.247 mol; acetic acid, 2.913 mol; methanol, 0.913 mol; water, 0.5516 mol; catalyst, 7.105 × 10^{-4} mol.

Operating Conditions			Reference
Temperature (K)	Pressure	CO Partial Pressure	
443 - 473	28 – 70 (bar)	11 – 56 (bar)	[20]
453 - 493	15 – 45 (atm)	2 – 30 (atm) , preferably: 4 – 15	[21-23]
453 - 493	15 – 40 (atm)	2 – 30 (atm) , preferably: 3 – 10	[24]

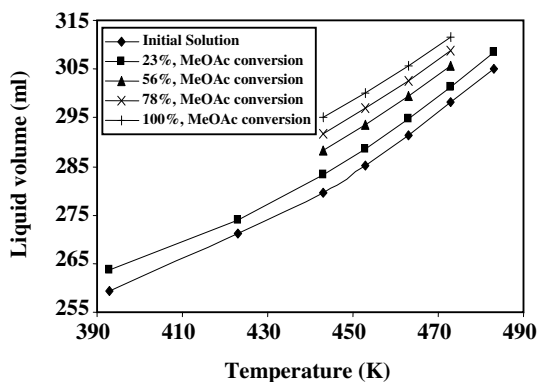*Fig. 10: Volume of the reaction mixture vs. temperature at the different methyl acetate conversions (calculated by the general NRTL-Virial model).*
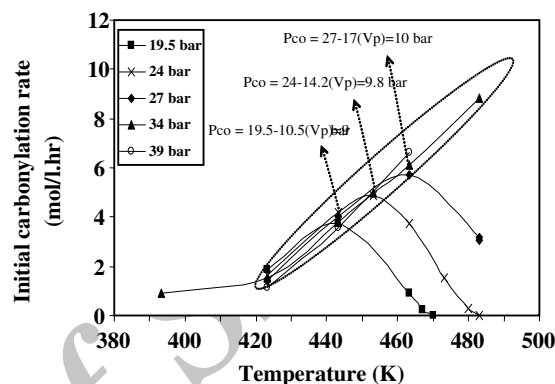

Fig. 11: Simultaneous effects of the operational condition and CO partial pressure on the initial rate of the carbonylation. Reaction conditions: methyl iodide, 0.247 mol; acetic acid, 2 mol; methyl acetate, 0.913 mol; water, 1.463 mol; catalyst, 7.105×10^{-4} mol.

The effect of CO partial pressure and temperature on the catalytic reaction rate

The normal operating range of carbonylation process reported in the literature [20-24] is presented in Table 3. According to the literature [21-24], the reaction temperature is approximately 423 to 523K.

Through the investigation of the volume changes of the reaction liquid in the autoclave by the general NRTL-Virial model, it is observed that the pressure has no significant effect on the volume of the reaction mixture. Fig. 10 shows these changes versus temperature at different conversions. In order to calculate the initial rate of the reaction at conversions below 20%, at constant temperatures, volume changes of the reaction mixture which are almost 1% according to Fig. 10, will be ignored.

At the end of the experiments, GC analysis of the liquid and gas phases was carried out which indicated the nearly complete conversion of methyl acetate with 99% selectivity to acetic acid. Traces (< 0.5%) of methane were detected in the gas phase and analysis of the gas phase showed less than 2% of CO_2 formation

by water-gas shift reaction. CO absorption versus time for low conversions (< 20%) was used for the calculation of the initial rates. It was observed that the reproducibility of the experiments was within ±5-7% which indicated that the experimental uncertainty is negligible.

Fig.11 shows that the rhodium catalyst in homogeneous methanol carbonylation media requires a certain temperature range for activation. Below the lower limit, 420K, the reaction does not occur at a commercially reasonable rate, and above upper limits at constant pressures, a decrease in the rate of reaction can be observed. Consequently, it is obtained that the reaction is kinetically and thermodynamically appropriate at temperatures above 420K and below 520K as shown in Fig. 8, respectively. This range of reaction temperature is in correspondence to that reported in the literature [21-24]. It is also observed that the rate of reaction in the dotted region is pressure-independent.

It is predicted that the solubility of CO in the solution is very low (It would be in the order of 10^{-1} mol/L, from the data reported by *Dake & Chaudhari* [25]), and

64

the activity coefficient of the solution is assumed very close to unity at low solubilities. Hence, CO partial pressure can be calculated from the total pressure (P), vapor pressure of the pure solution (P*, measured and shown in Fig. 5) and the mole fraction of dissolved carbon monoxide (x, which is minor) with the aid of Raoult's law. Thus, the CO partial pressure (P_{CO}) is given by:

$$P_{CO} = P - P*(1-x) \approx P - P* \tag{15}$$

As seen in Fig. 11, the temperatures of the maximum rate points at total pressures 19.5, 24, and 27 bar are 443, 453, and 463K, respectively. At these points, if the vapor pressures of the initial reaction mixture shown in Fig. 5, 10.5, 14.2, and 17 bar, respectively, are deducted from the corresponding total pressures, according to Eq. (15), it is estimated that the CO partial pressure varies from 9 to 10 bar. At temperatures below the maximum rate temperatures, with the $P_{CO} > 9$ - 10 bar, the reaction rate is independent of the pressure. Consequently, the reaction rate is independent of the CO partial pressure above approximately 10 bar as reported by *Dake et al.* [10] ($P_{CO} > 10$ bar at T = 423, 433, and 444K). It is also observed from Fig. 11 that the decrease in rate of reaction with an increase in the temperature at constant total pressures, is due to the reduction in CO partial pressure which changes the rate-determining step (ligand addition step at $P_{CO} < 10$ bar and oxidative addition at $P_{CO} > 10$ bar) [10]. Fig. 11 shows that the rate is zero at 19.5 and 24 bar total pressures at 470 and 483K temperatures, respectively. As shown in Fig. 5, vapor pressures of the initial reaction mixture at 470 and 483K are 17.5 bar and 22 bar, respectively. Thus, in accordance with Eq. (15), the minimum amount of CO pressure to initialize the reaction is above 2 bar. It was observed in this case, if the minimum amount of CO is not satisfied, precipitating and hence deactivating of the catalyst will occur. Enough CO addition or temperature decrease results in catalyst reactivation. The catalyst precipitation (RhI_3) in the pristine industrial carbonylation process (Monsanto) has been observed in CO deficient areas of the plant (see chemical equations. (16) and (17)) [15].
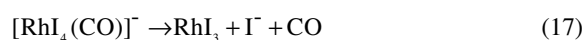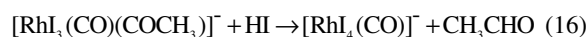
$$[RhI_3(CO)(COCH_3)]^- + HI \rightarrow [RhI_4(CO)]^- + CH_3CHO \tag{16}$$

$$[RhI_4(CO)]^- \rightarrow RhI_3 + I^- + CO \tag{17}$$

Fig. 11 is useful to realize the CO partial pressure-independent behavior of the experiments to determine the intrinsic rate constant. It should be noted that for commercial utility, the deactivation rate must be as low as possible dictating the maximum temperature of the reaction [26]. Determination of maximum operating temperature requires a more detailed study beyond the scope of this paper.

As it was noted before, the use of metal salts in low contents (ca. 0.3 - 4 wt. %) as new promoters in carbonylation process has been proposed [6-8]. There is a strong possibility that the promoters may influence the way that the pressure and CO partial pressure affect the rate of reaction. This subject is under investigation.

Determination of the equilibrium, rate and Henry's law constants

The Density Functional Theory (DFT) previously used in methanol carbonylation [27-30] with the hybrid B3LYP exchange and correlation functional [31,32] is used to obtain the K_2, K_3, K_4, and K_5 equilibrium constants (see Eq. (6)) under Effective Core Potential (ECP) approximation [33]. The geometries of the reactants, intermediates, transition states and the product for carbonylation catalyzed by cis-$[Rh(CO)_2I_2]^-$, as shown in Fig. 3, were optimized by B3LYP/SDD level chemistry. The SDD basis set includes D95V for carbon, oxygen and hydrogen atoms. The Stuttgart/Dresden effective core potentials along with the scalar relativistic corrections have been used for rhodium and the halogen. Changes of the Gibbs free reaction energy (ΔG) of the gas phase were calculated considering zero-point energies, thermal motion, and entropy contributions at 443, 463, and 473K temperatures under 34 bar pressure. All of the calculations were performed using Gaussian 98 suite program package [34]. The theoretical results of the equilibrium constants were fitted with temperature and are presented in Table 4.

It should be noted that to calculate the thermodynamic properties from the computational calculations, there are different Level Chemistries such as DFT, Post-HF (MP2, MP4, …), HF and etc. From which the DFT method as one of the most up to date and developed ones in the recent decade was used in our study. Among basis functions, SDD was chosen thanks to its closeness to our studied catalysis cycle (Fig. 3), though other basis functions such as LANL2DZ could be used.

65

Table 4: Equilibrium constants of the migration (K_2), ligand addition (K_3), reductive elimination (K_4) and the production release reaction (K_5) steps estimated by Gaussian 98 suite program package. ($\Delta G = \Delta H - T\Delta S$, $K = exp(-\Delta G/RT)$).

Equilibrium constants	T(K)			Logarithmic function of the equilibrium constants
	443	463	473	
K_2	691686.40	407022.90	317310.80	$3.19 \exp(45266.15/RT)$
K_3	5.06	2.60	1.91	$(1.08 \times 10^{-6}) \exp(56588.12/RT)$
K_4	1844.74	2432.90	2761.26	$(1.07 \times 10^{6}) \exp(-23435.92/RT)$
K_5	179473.90	111566.20	89387.83	$3 \exp(40525.22/RT)$

Table 5: Initial rates of the carbonylation reaction of methanol at 34 bar. Reaction conditions: methyl iodide, 0.247 mol; acetic acid, 2 mol; methyl acetate, 0.913 mol; water, 1.463 mol; catalyst, 7.105 × 10-4 mol.

No.	[AcOH](mol/l)	[MeOAc](mol/l)	[H$_2$O](mol/l)	[Rh]*10^4(mol/l)	[CH$_3$I](mol/l)	X	P$_{CO}$(kPas)	T(K)	Rate(mol/l.hr)
1	7.16	3.27	5.23	25.33	0.88	0	2156	443	3.8
2	7.29	3.21	5.17	25.33	0.88	0.02	2168	443	3.79
3	7.42	3.14	5.10	25.33	0.88	0.04	2180	443	3.78
4	7.55	3.08	5.04	25.33	0.88	0.06	2191	443	3.76
5	7.68	3.01	4.97	25.33	0.88	0.08	2203	443	3.74
6	7.81	2.95	4.91	25.33	0.88	0.1	2214	443	3.74
7	7.94	2.88	4.84	25.33	0.88	0.12	2225	443	3.73
8	8.07	2.82	4.78	25.33	0.88	0.14	2236	443	3.72
9	8.20	2.75	4.71	25.33	0.88	0.16	2246	443	3.71
10	8.33	2.69	4.65	25.33	0.88	0.18	2257	443	3.69
11	6.87	3.13	5.02	24.41	0.85	0	1730	463	6.14
12	7.08	3.03	4.92	24.41	0.85	0.03	1753	463	6.11
13	7.28	2.92	4.81	24.41	0.85	0.07	1783	463	6.09
14	7.49	2.82	4.71	24.41	0.85	0.1	1804	463	6.09
15	7.69	2.72	4.61	24.41	0.85	0.13	1826	463	6.06
16	7.90	2.62	4.51	24.41	0.85	0.16	1847	463	6.04
17	8.10	2.51	4.40	24.41	0.85	0.2	1873	463	6.03
18	6.71	3.06	4.91	23.59	0.82	0	1483	473	7.39
19	6.95	2.94	4.79	23.59	0.82	0.04	1517	473	7.4
20	7.20	2.82	4.67	23.59	0.82	0.08	1550	473	7.38
21	7.44	2.69	4.54	23.59	0.82	0.12	1582	473	7.35
22	7.69	2.57	4.42	23.59	0.82	0.16	1613	473	7.32

To determine the solubility of CO in liquid mixture, Henry's law was used as Eq. (18).

$$[CO] = H_{co} \times P_{CO} \qquad (18)$$

Henry's coefficient for CO (H_{CO}) at different methyl acetate conversions (X) and temperatures (T) was determined by using equation (19), previously used by *Dake & Chaudhari* [25]:

$$\ln(H_{CO}) = A + \frac{B}{T} + C(X)(\frac{1}{T}) + E\ln(1+X) \qquad (19)$$

To calculate the partial pressure of CO (P$_{CO}$) at different methyl acetate conversions and temperatures in the autoclave, the vapor pressure of the reaction solution

(P*) was measured (shown in Fig. 5). P* in kPas is expressed by:

$$P^* = 8615.172 - 39.328\ T - 420.331\ X + \qquad (20)$$
$$2.18 \times 10^{-2}\ T^2 - 722.412\ X^2 + 7.38\ X\ T + 6.64 \times 10^{-5}\ T^3 -$$
$$126.03\ X^3 + 2.27\ T\ X^2 - 1.76 \times 10^{-2}\ X\ T^2$$

By studying (i) the rates of the carbonylation reaction conducted at 443, 463, and 473K under 34-bar pressure, (ii) CO partial pressures from Eqs. of (15) and (20), (iii) determined concentrations of the components during the reaction based on the stoichiometry of the overall reaction presented in Table 5 and (iv) the equilibrium constants obtained by Gaussian 98 presented in Table 4, the parameters involved in the non-linear rate Eq. (13)

Table 6: The Arrhenius parameters of the rate constant for the carbonylation.

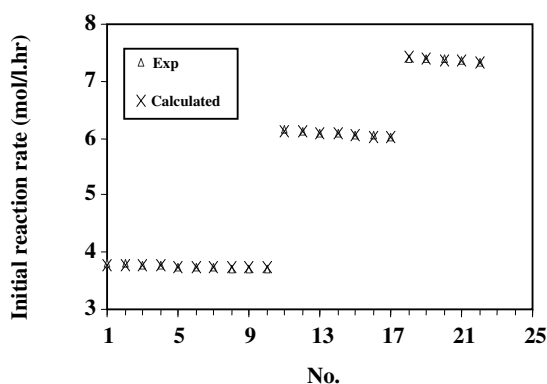| Parameters	This work	*Nowicki et al.* [11] (raw data) (1992)	*Nowicki et al.* [11] (corrected data) (1992)	*Dake et al.* [10] (1989)	*Hjortkjaer & Jensen* [17] (1976)
$10^{-6} \times k_{\circ}$	859.412 (L/mol. h)	16200 (L/mol. h)	571680 (L/mol. h)	14 (L^2/mol^2.h)	12600 (L/mol^2. h)
E, kJ/mol	48.271	61.2	72.2	68.5	61.7
T, K	443-473	443-470	443-470	423-443	423-498
P, bar	34	22-50	22-50	$P_{CO} > 10$	-

Fig. 12: Comparison of the experimental and calculated initial reaction rates.

accompanied with Eqs. (6), (18) and (19) were estimated via non-linear regression method. Due to the reliability of the rate Eq. (13) in water contents more than 8 wt. % - the chemical Eq. (12) consumes water, the data of the initial rates were used to calculate the parameters. The data reported by *Dake & Chaudhari* [25] and proposed by the general NRTL-Virial model were used to provide initial guesses for the constants of Eq. (19) and K′K″, respectively. There is a good agreement between the experimental and calculated rates as shown in Fig. 12. The errors between the predicted and experimental rates were found to be ±%1. Consequently:

$$k = 859.412 \times 10^6 \exp(-48271.525 / R\,T) \quad (21)$$

$$K'K'' = 6.551 \times 10^{-1} \exp(2044.439 / T) \quad (22)$$

$$\ln(H_{CO}) = -7.2 - \frac{905.493}{T} - 237.533(X)(\frac{1}{T}) - \quad (23)$$
$$0.366\ln(1+X)$$

It should be noted that the calculated activation energy of the reaction (48.271 kJ/mol) is almost the same as the reported experimental results (50 - 71 kJ/mol [28]).

Table 6 shows a comparison of the pre-exponential factors ($k_{\circ}$) and the activation energies (E) calculated in the present work with those found in the literature. The reaction rates given by *Nowicki et al.* [11] have been calculated according to temperature from Eq. (4), and the pressure of none of the tests is clear. The corrected parameters in the work of *Nowicki et al.* [11] (see Table 6) have been determined on the basis of their result that methyl iodide is almost equimolarly distributed between the gaseous and liquid phases, but with regard to our studies by using the general NRTL-Virial model, it was clear that almost all of the methyl iodide remains in the liquid phase, reaction phase, in the pressures above 20 bar at the reaction temperatures. In addition, when water is used as the solvent, the methyl iodide is distributed between the gaseous and the liquid phases depending on the vapor-liquid equilibrium [10], but *Nowicki et al.* used acetic acid as the solvent which methyl iodide is infinitely soluble in it [10].

Besides, by using the general NRTL-Virial model, it was found that at the beginning of the reaction (at 19.5 - 39 bar and 393 - 483K) the weight of vapor phase in the reactor headspace volume is 4.5 - 7.5 grams. It was also found that nearly 25 - 85 wt. % is liquid contents (i.e., ~ 1 - 2.5 wt. % of the initial charge). This amount of change in the initial charge of the liquid phase will not be caused to any worth mentioning error in the kinetic study.

As it may be seen from Table 6, the activation energy given by *Dake et al.* [10] determined at 423 - 443K is higher than those obtained by other authors. The normal operating range as cited in the patents is 443 to 473K [20]. At these conditions, it is observed from Fig. 11 that the reaction rate is more commercially reasonable.

Unfortunately, *Hjortkjaer & Jensen* [17] have not precisely described the pressure conditions of any of the tests to calculate the values of the reaction rate parameters from Eq. (4). On the basis of Hjortkjaer and Jensen's finding that the carbonylation rate is
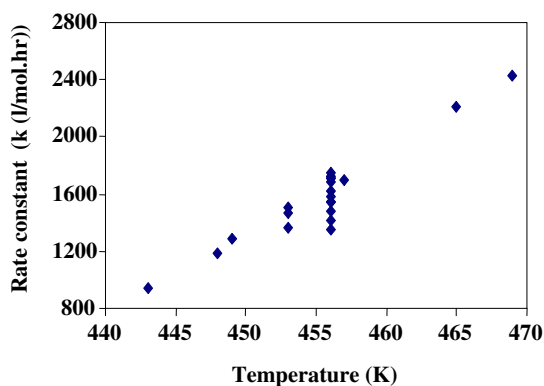
Fig. 13: The reaction rate constants (k) achieved from the reported raw data by Nowicki et al. (Nowicki et al., 1992).

independent of the CO partial pressure above approximately 2 atm, their reported parameters may not be inherent.

As it is seen in Fig. 11, in a constant pressure the reaction rate is affiliated to the CO partial pressure above a specific temperature. In this region, the reaction rate decreases with increasing the temperature. Therefore, without paying attention to the CO partial pressure independency, it may lead to lower rate constant (k) than the real value. Furthermore, in experiments run under different total pressures at a constant temperature, with no regard to the CO partial pressure independency, different rate constants are found that are related to two different rate-controlling steps. It is observed in Fig. 13 based on the reported raw data by *Nowicki et al.* [11] that this fact is not noticed at 453 and 456K temperatures. Therefore, according to the above mentioned issues and their saying that the partial pressure of CO has no direct effect on the reaction rate above 2 bar, their reported parameters can not be inherent.

Additionally, at the high pressures (P = 30 and 40 bar), it is clear from Fig. 9 that the equilibrium proceeding of the esterification reaction is almost independent of pressure and it can proceed to the right at temperatures below 520K without any significant restriction, but at lower pressures, at temperatures above 463K the proceeding of the reaction is dependent on the pressure and temperature. In the last operating conditions, after warming the entering reaction mixture into the reactor, different amounts of methyl acetate and water are produced with respect to pressure and temperature.

Consequently, the assumption of equality of the initial reaction mixture under different operating conditions cannot still hold in kinetic studies here. However, this result may not seem so troubling in carbonylation in acidic media due to the facts that (i) the reaction rate is independent of methyl acetate at contents above ~ 1 wt. % [15] and not affected by methanol concentration (reported by Dake et al. [10]) and also (ii) the methanol is first converted to methyl acetate and water through esterification with acetic acid and then carbonylated.

Additionally, the concentration of methyl iodide could possibly change in accordance with the chemical equilibrium Eq. (2) [10]. The difference in kinetics can be attributed to changes in the concentration of methyl iodide as the only reactant which directly affects the reaction rate in the bulk liquid due to the thermodynamic restrictions i.e. solubility, vapor-liquid equilibria and chemical equilibrium. As it was noted, solubility of methyl iodide and its vapor-liquid equilibrium are not among thermodynamic restrictions in the kinetic studies of carbonylation system in acidic media. Moreover, it has been found that the equilibrium constant of the reaction strongly favors methyl iodide [35].

Considering the results, it can be concluded that the effects of the chemical equilibriums under different operating conditions in our kinetic studies can be safely assumed negligible.

Comparison of the predicted CO solubility with that proposed by the general NRTL-virial model

Dake & Chaudhari [25] have reported CO solubility data over a wide range of temperatures (298K to 448K) and pressures (10 bar to 80 bar) in different aqueous mixtures. *Kelkar et al.* [36] have obtained the solubility data for CO in acetic acid, methyl acetate, and acetic acid/methyl acetate mixtures in the temperature range of 433 - 463K at 4.7 - 55 bar partial pressure of CO.

By comparing the CO solubility data predicted by Eqs. (15), (18), (20) and (23) with those resulted by the general NRTL-Virial model presented in Table 7, the agreement was found to be excellent, with the errors below 11%, even at high conversions where the water content is lower than 8 wt. %, suggesting that the proposed formula here for CO solubility can be reliably used for design and scale up purposes. As expected, the solubility of CO in the reaction solution is in the order of 10^{-1} mol/L.

Table 7: Comparison of the predicted CO solubility with that proposed by the general NRTL-Virial model under 34-bar pressure.

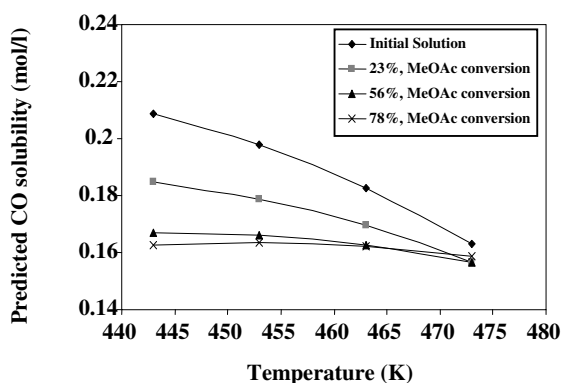| MeOAc Conversion	[CO] (mol/l)							
	443K		453K		463K		473K	
	predicted	model	predicted	model	predicted	model	predicted	model
0	0.2085	0.1967	0.1977	0.1842	0.1827	0.1702	0.1632	0.1469
0.23	0.1850	0.1869	0.1789	0.1798	0.1695	0.17	0.1566	0.1532
0.56	0.1669	0.1724	0.1659	0.1704	0.1625	0.1667	0.1565	0.1556
0.73	0.1628	0.1628	0.1635	0.1616	0.1621	0.1612	0.1586	0.1544

Fig. 14: Predicted CO solubility data vs. temperature at different methyl acetate (MeOAc) conversions in the reaction mixture under 34-bar pressure. (Initial solution): methyl iodide, 0.247 mol; acetic acid, 2 mol; methyl acetate, 0.913 mol; water, 1.463 mol; catalyst, 7.105 × 10⁻⁴ mol.

In Fig. 14, it is observed that for all of the conversions studied, the predicted solubility of CO decreases with increasing the temperature. Furthermore, with the reaction proceeding, a considerable decrease in the effect of temperature on solubility of CO is seen. It should, however, be noted that the solubility of CO in acetic acid, methyl acetate and acetic acid/methyl acetate mixtures reported by *Kelkar et al.* [36] and acetic acid/water obtained by *Dake & Chaudhari* [25] increases with increasing temperature. This difference is presumably due to the presence of methyl iodide in our studied mixture.

As seen in Fig. 14, the increase in acetic acid concentration and subsequently the decrease in water and methyl acetate concentrations; in other words, the proceeding of the reaction decreases the CO solubility which is more obvious at temperatures below 470K. Considering the data reported by *Kelkar et al.* [36], it was found that CO is more soluble in methyl acetate than

in acetic acid, and an increase in acetic acid concentration or a decrease in methyl acetate concentration in the acetic acid/methyl acetate mixture leads to a decrease in the solubility of CO, which is in good agreement with those obtained here.

It is also obvious from Fig. 14 that in low conversions (< 23 %), the solubility changes of CO with the proceeding of the reaction and temperature is considerable. Consequently, for kinetic studies and determination of the intrinsic rate constant, using Eq. (13) instead of equation (4) that is independent of CO partial pressure is the most appropriate. It is clear from Fig. 14 that at high temperatures, the solubility of CO does not change sharply with the change of the concentrations.

Modeling and simulation

In order to model and predict the rate-time, concentration-time and the CO consumption-time profiles in a batch reactor at temperatures 443, 463 and 473K under 34-bar pressure, Eq. (13) accompanied with algebraic Eqs. (6), (15), (18), (20) to (23) and also Eq. (12) as the total reaction ($Rate_{CH3COOH}$ = $-Rate_{CH3COOCH3}$ = $-Rate_{H2O}$ = $-Rate_{CO}$), initial concentrations presented in Table 5 (at X = 0), and functions of the equilibrium constants presented in Table 4 were solved numerically using the implicit Euler method.

Volume changes during the reaction which is about 4 to 5.5% at constant reaction temperatures (443 - 473K) will be ignored according to Fig. 10.

In order to simulate the reaction under 34 bar, the commercial dynamic simulator HYSYS.Plant was run using the general NRTL-Virial property package with the binary interaction parameters from Table 2 and the mixing rule in Eq. (14). Using the definition of Eq. (13) as the reaction rate expression whose its form is similar to

69

the heterogeneous catalytic reaction kinetics model provided by the simulator and the Eqs. (21) and (23) as the functions of the equilibrium constants presented in Table 4 along with Eq. (12) as the total reaction in the 450 cm^3 reactor as described in experimental section, the reaction will be simulated. Since the effect of catalyst on the vapor pressure of the reaction mixture at different methyl acetate conversions and temperatures (shown in Fig. 6) is negligible, the solid catalyst does not take part in VLE calculations in simulation media, and its vapor pressure information is, by default, set to zero. Hysys was used to solve all of the equations using the fully implicit Euler integration method.

By comparing the experimental data with the results of modeling and simulation shown in Figs. 15 - 17, the agreement was found to be excellent even in water contents lower than 8 wt. % (that at the end of the reaction, it is almost 3.6 wt. %), which suggests that the determined parameters, equilibrium constants, CO solubility and rate constant, can be reliably used for design and scale up purposes.

Due to the decline in the concentration of substrate, product inhibition and binding up to catalyst, the fraction of active catalyst decreases and thus the reaction rate reduces (see Fig. 16) [26].

An experiment was run at 34 bar and 453K under the conditions described in Table 1 and compared with modeling and simulation results. As shown in Fig. 18, it is found that the determined parameters produce satisfactory results.

CONCLUSIONS

By reviewing the courses of on research the methanol carbonylation in the field of kinetic studies, it was revealed that the lack of the adequate thermodynamic studies and sufficient precision in the study of the simultaneous effects of operation conditions (temperature and partial pressure) has only led to the determination of the apparent rate constant and not the inherent constant.

This study leads to an efficient and simultaneous estimation of the effects of pressure, temperature, and the thermodynamic restrictions on kinetic investigation of the homogeneously rhodium catalyzed carbonylation process and the determination of its intrinsic rate constant.

It was found that the general NRTL-Virial model is identified as a proper fluid property package for
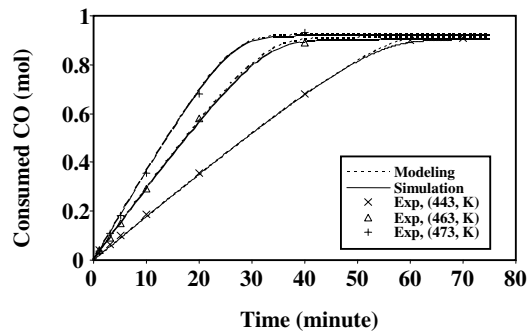

Fig. 15: Comparison of CO consumed in the experimental runs with those proposed in modeling and simulation under 34-bar pressure. Reaction conditions: methyl iodide, 0.247 mol; acetic acid, 2 mol; methyl acetate, 0.913 mol; water, 1.463 mol; catalyst, 7.105 × 10^{-4} mol.
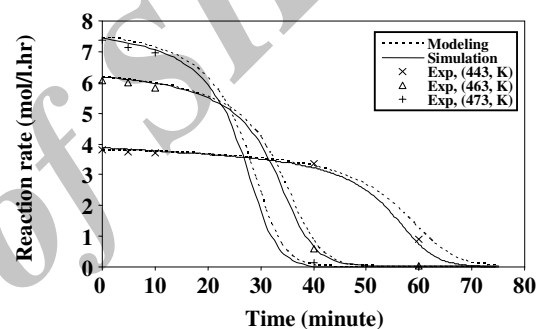

Fig. 16: Comparison of the experimental reaction rate with those proposed in modeling and simulation under 34-bar pressure. Reaction conditions: methyl iodide, 0.247 mol; acetic acid, 2 mol; methyl acetate, 0.913 mol; water, 1.463 mol; catalyst, 7.105 × 10^{-4} mol.
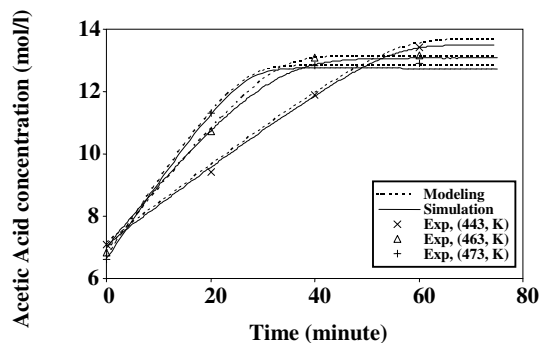

Fig. 17: Comparison of the experimental Acetic acid concentration with those proposed in modeling and simulation under 34-bar pressure. Reaction conditions: methyl iodide, 0.247 mol; acetic acid, 2 mol; methyl acetate, 0.913 mol; water, 1.463 mol; catalyst, 7.105 × 10^{-4} mol.
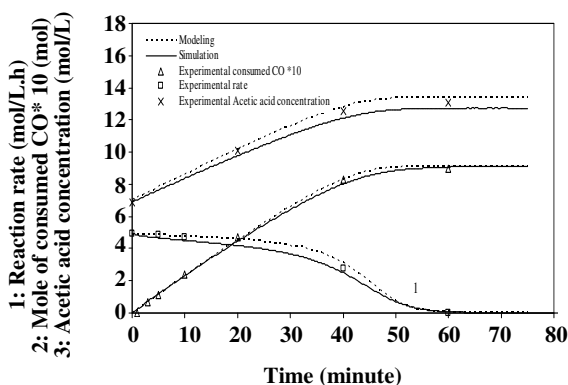
70

Fig. 18: Comparison of data of the experiment conducted at 34-bar and 453K with those proposed in modeling and simulation. Reaction conditions: methyl iodide, 0.247 mol; acetic acid, 2 mol; methyl acetate, 0.913 mol; water, 1.463 mol; catalyst, 7.105 × 10^{-4} mol.

carbonylation system. It was also concluded that the equality of the initial reaction mixture under the different operating conditions in the kinetic studies is a correct assumption. We explained how the reaction is reasonable at the $T > 420K$ and $T < 520K$ from the reaction rate and thermodynamic equilibrium points of view, respectively. This range of reaction temperature was in good agreement with that reported in the literature.

In addition, the determination of reaction rate parameters through the kinetic study and the ab initio method using the Gaussian 98 program led to the determination of a CO solubility expression for rhodium catalyzed methanol carbonylation. The Density Functional Theory (DFT) with the hybrid B3LYP exchange and correlation functional was used to obtain the equilibrium constants under Effective Core Potential (ECP) approximation. A good agreement was found between the CO solubility predicted here with the results of the general NRTL-Virial model.

It was observed that an increase in acetic acid or a decrease in methyl acetate concentrations leads to a decrease in the solubility of CO. The results are in good agreement with that obtained by others. It was also found that the reaction rate parameters determined here give satisfactory predictions in modeling and simulation of the reaction.

Nomenclature

A_{ij}	Non-temperature dependent energy parameter between components i and j
AcOH	Acetic acid
B_{ij}	Temperature dependent energy parameter between components i and j
E	Activation energy, kJ/mol
H_{CO}	Henry's constant of CO, mol/L kPa
[I]	Promoter concentration, mol/L
$[I]_t$	Total amount of promoter, mol/L
k	Reaction rate constant, mol/l h
$K_2, K_3, K_4, K_5, K', K''$	Equilibrium constants
MeOAc	Methyl acetate
MeOH	Methanol
n	Total number of components
P	Total pressure
P_{CO}	Partial pressure of carbon monoxide, kPa
P*	Vapor pressure of the reaction solution, kPa
R	Universal gas constant, 8.314 J/mol K
Rate	Reaction rate, mol/L h
[Rh]	Total amount of rhodium catalyst, mol/L
t	Time, minute
T	Temperature, K
x	Mole fraction of dissolved carbon monoxide
x_i	Mole fraction of component i
X	Methyl acetate conversion
[Y]	Concentration of the species Y, mol/L
α_{ij}	NRTL non-randomness constant for binary interaction, note that $\alpha_{ij} = \alpha_{ji}$ for all binaries
γ_i	Activity coefficient of component i
ΔG	Change in Gibbs free energy
ΔH	Change in enthalpy
ΔS	Change in entropy

REFERENCES

[1] Von Kutepow N., Himmle W., Hohenschutz H., Die Synthese Von Essigsäure Aus Methanol und Kohlenoxyd, *Chemie Ingenieur Technik*, **37** (4), p. 383 (1965).

[2] Paulik F.E., Roth J.F., Novel Catalysts for the Low-Pressure Carbonylation of Methanol to Acetic Acid, *Chem. Commun*, 1578a (1968).

71

[3] Roth J.F., Craddock J.H., Hershman A., Paulik F.E., Low Pressure Process for Acetic Acid Via Carbonylation, *Chem. Techn*, **1**, p. 600 (1971).

[4] Murphy M.A., Smith B.L., Torrence G.P., Aguilo A., Iodide and Acetate Promotion of Carbonylation of Methanol to Acetic Acid: Model and Catalytic Studies, *J. Organomet. Chem,* **303**, p. 257 (1986).

[5] Smith B.L., Torrence G.P., Murphy M.A., Aguilo A., The Rhodium-Catalyzed Methanol Carbonylation to Acetic Acid at Low Water Concentrations: the Effect of Iodide and Acetate on Catalyst Activity and Stability, *J. Mol. Catal,* **39** (1), p. 115 (1987).

[6] Qian Q., Li F., Yuan G., Promoting Effect of Phosphates Upon Homogeneous Methanol Carbonylation, *Catal. Commun*, **6**, p. 446 (2005).

[7] Zhang S., Qian Q., Yuan G., Promoting Effect of Transition Metal Salts on Rhodium Catalyzed Methanol Carbonylation, *Catal. Commun*, **7**, p. 885 (2006).

[8] Qian Q., Zhang S., Yuan G., Promoting Effect of Oxometallic Acids, Heteropoly Acids of Mo, W and Their Salts on Rhodium Catalyzed Methanol Carbonylation, *Catal. Commun*, **8**, p. 483 (2007).

[9] Maitlis P.M., Haynes A., Sunley G.J., Howard M.J., Methanol Carbonylation Revisited: Thirty Years on, *J. Chem. Soc, Dalton Trans,* **11**, p. 2187 (1996).

[10] Dake S.B., Jaganathan R., Chaudhari R.V., New Trends in the Rate Behavior of Rhodium-Catalyzed Carbonylation of Methanol, *J. Ind. Eng. Chem. Res,* **28**, 1107 (1989).

[11] Nowicki L., Ledakowicz S., Zarzycki R., Kinetics of Rhodium-Catalyzed Methanol Carbonylation, *Ind. Eng. Chem. Res*, **31**, 2472 (1992).

[12] Kim J.S., Ro K.S., Woo S.I., Computer Simulation of Reaction Rate Expression for Methanol Carbonylation Reaction Catalyzed Over RhCl$_3$-3H$_2$O/HI, *J. Mol. Catal,* **69**, 15 (1991).

[13] Forster D.J., On the Mechanism of a Rhodium-Complex-Catalyzed Carbonylation of Methanol to Acetic acid, *J. Am. Chem. Soc*, **98**, 846 (1976).

[14] Forster D.J., Mechanistic Pathways in the Catalytic Carbonylation of Methanol by Rhodium and Iridium Complexes, *Adv. Organomet. Chem*, **17**, 255 (1979).

[15] Jones J.H., The Cativa^{TM} Process for the Manufacture of Acetic acid, *Platinum metals Rev*, **44** (3), 94 (2000).

[16] Tonde S.S., "Carbonylation of Alcohols and Olefins Using Soluble Transition Metal Catalysts", Ph.D. Dissertation, Homogeneous Catalysis Division National Chemical Laboratory, University of Pune, Pune, (2004) [Online]. Available: http://dspace.ncl.res.in/dspace/bitstream/2048/138/1/th1382.pdf

[17] Hjortkjaer J., Jensen V.W., Rhodium Complex Catalyzed Methanol Carbonylation, *Ind. Eng. Chem. Prod. Res. Dev,* **15** (1), p. 46 (1976).

[18] Kelkar A.A., Ubale R.S., Deshpande R.M., Chaudhari R.V., Carbonylation of Methanol Using Nickel Complex Catalyst: a Kinetic Study, *J. Cata,* **156**, p. 290 (1995).

[19] HYSYS 3.2 simulation basis, Hyprotech Ltd., Calgary, Canada, (2003) [Online]. Available: http://yunus.hacettepe.edu.tr/~ealper/kmu346/tutorial/SimBasis.pdf

[20] James J.L.M., Jeffrey C.F.C., Acetic Acid by Low Pressure Carbonylation of Methanol, PEP Review 78-3-4. (1980) [Online abstract]. Available: http://www.sriconsulting.com/PEP/Public/Reports/Phase_78/RW78-3-4/

[21] Smith B.L., Torrence G.P., Aguilo A., Alder J.S., Methanol Carbonylation Process, *U.S. Patent 5,026,908*, (1991).

[22] Smith, B.L., Torrence, G.P., Aguilo, A., Alder, J.S., Methanol Carbonylation Process, *U.S. Patent 5,001,259*, (1991).

[23] Smith B.L., Torrence G.P., Aguilo A., Alder J.S., Methanol Carbonylation Process, *U.S. Patent 5,144,068*, (1992).

[24] Trueba D.A., Kulkarni S., Control Method for Process of Removing Permanganate Reducing Compounds from Methanol Carbonylation Process, *U.S. Patent 7,271,293*, (2007).

[25] Dake S.B., Chaudhari R.V., Solubility of CO in Aqueous Mixtures of Methanol, Acetic Acid, Ethanol, and Propionic acid, *J. Chem. Eng. Data,* **30**, p. 400 (1985).

[26] Garland M., Transport Effects in Homogeneous Catalysis, In "Encyclopedia of Catalysis", Horvath I.T., Ed.; Wiley: Eötvös university, Budapest, Hungary, Vol. **3**, pp. 480-490 (2003).

[27] Ming L., Wenlin F., Maorong H., Yongqiang J., Zhenfeng X., Ab initio study on the Mechanism of Rhodium-Complex Catalyzed Carbonylation of Methanol to Acetic acid, *Sci China Ser B-Chem*, **44** (5), p. 465 (2001).

[28] Kinnunen T., Laasonen K., DFT-Studies of Cis- and Trans-[Rh(CO)$_2$X$_2$]$^+$ (X=/PH$_3$, PF$_3$, PCl$_3$, PBr$_3$, PI$_3$ or P(CH$_3$)$_3$) and Oxidative Addition of CH$_3$I to Them, *J. Organomet. Chem*, **665**, p. 150 (2003).

[29] Ivanova E.A., Nasluzov V.A., Rubaylo A.I., Rösch N., Theoretical Investigation of the Mechanism of Methanol Carbonylation Catalyzed by Dicarbonyldiiodorhodium Complex, *Chemistry for Sustainable Development*, **11**, p. 101 (2003).

[30] Maorong H., Wenlin F., Yongqiang J., Ming L., IRC Analysis of Methanol Carbonylation Reaction Catalyzed by Rhodium Complex, *Sci China Ser B-Chem*, **47** (1), p. 41 (2004).

[31] Lee C., Yang W., Parr R.G., Development of the Colle-Salvetti Correlation-Energy Formula into a Functional of the Electron Density, *Phys. Rev. B*, **37**, p. 785 (1988).

[32] Becke A.D., Density-Functional Thermochemistry. III. The Role of Exact Exchange, *Chem. Phys*, **98** (7), p. 5648 (1993).

[33] Hay P.J., Wadt W.R., Ab Initio Effective Core Potentials for Molecular Calculations. Potentials for the Transition Metal Atoms Sc to Hg, *Chem. Phys*, **82** (1), p. 270 (1985).

[34] Frisch M.J., Trucks G.W., Schlegel H.B., Scuseria M.A., Robb M.A., Zakrzewski V.G., Montgomery J.A., Stratman R.E., Burant J.C., Daprich S., Millam J.M., Daniels A.D., Kudin K.N., Strain M.C., Farkas O., Tomasi J., Barone V., Cossi M., Cammi R., Mennucci B., Pomelli C., Adamo C., Clifford S., Ochterski J., Petersson G.A., Ayal P.Y., Ciu Q., Morokuma K., Malick D.K., Rabuck A.D., Raghavachari K., Foresman J.B., Cioslowski J., Oritz J.V., Stefanov B.B., Liu G., Liashenko A., Piskorz P., Komaromi I., Gomperts R., Martin R.L., Fox D.J., Keith T.A., Al-Laham M.A., Peng C.Y., Nanayakkara A., Gonzales C.A., Challacombe M., Gill P.M.W., Johnson B.G., Chen W., Wong M.W., Andres J.L., Head-Gordon M., Replogle E.S., Pople J.A., Gaussian 98, Revision A.7, Gaussian, Inc.: Pittsburgh, PA (1995).

[35] Forster D., Advances in Organometallic Chemistry, In: "Catalysis and Organic Syntheses", Stone F.G.A., West R., Eds.; Academic Press: New York, San Francisco, London, Vol. **17**, pp. 262 (1979).

[36] Kelkar, A.A., Jaganathan, R., Chaudhari, R.V., Hydrocarbonylation of Methyl Acetate Using a Homogeneous Rh(CO)Cl(PPh$_3$)$_2$ Complex as a Catalyst Precursor: Kinetic Modeling, *Ind. Eng. Chem. Res*, **40**, 1608 (2001).